Modelling thin film solar cells with graded band gap

Koen Decock[1], Johan Lauwaert[1,2] , Marc Burgelman[1]
[1]Department of Electronics and Information Systems (ELIS), University of Gent,
St-Pietersnieuwstraat 41, B-9000 Gent, Belgium, Koen.Decock@Elis.Ugent.be
[2]Department of Solid State Sciences, University of Gent, Krijgslaan 281-S1, B-9000 Gent, Belgium

***Abstract* – This paper discusses how graded absorber structures in CIGS-based solar cell can be studied using the numerical simulation tool SCAPS. A model will be built for an AVANCIS solar cell with double grading which is produced with the laboratory line process. We will first discuss how literature and measurement data should be used to start the buildup of the model and afterwards give an illustration how the model then still has to be optimized. We will draw special attention to the consequences of a graded structure on the model. Moreover, we will show how one can discern the real grading benefit by comparison with a uniform reference model.**

1 INTRODUCTION

Using material systems such as CIGS it is possible to produce solar cells where the band gap changes throughout the absorber layer. Introducing a 'grading' in the absorber can improve cell performance [1] and some modern CIGS-solar cells already have such a graded band gap profile [2]. It is however difficult to discern the real benefit of grading, as varying material properties through the cell implies changing the mean value of the studied parameter, and it is almost impossible to produce a reference cell having the same properties as the studied cell, but with a uniform layout. Hence if one wants to study grading properties thoroughly one should use numerical simulation. Several authors have already performed simulations of graded solar cells [3], [4], [5]. Usually one starts from a 'typical' solar cell structure, but in order to improve the validity of the simulation it is desirable that the model mimics a real solar cell. The catch however lies in the fact that a realistic model depends on an enormous number of parameters, and it should be able to reproduce a variety of measurements [6]. In this work we will show how such a realistic model can be constructed using SCAPS, a solar cell simulation tool of the University of Gent available to the PV research community [7]. Version 2.8 can handle graded cell structures [8]. We start from literature data and measurements performed on an AVANCIS solar cell which is produced with the laboratory line process. This cell exhibits a double grading profile [2]. *C-V*, *C-f* and *I-V* measurements were performed at different temperatures next to spectral response and DLTS measurements. Special attention will be drawn to the consequences of grading on the model. Moreover we will show how we afterwards can discern the real grading benefit by comparison with a uniform reference model.

2 DATA FROM LITERATURE

It is impossible to explore the entire parameter space describing a solar cell. A typical model consists of approximately 6 layers. When each layer has one defect, one already needs over 120 parameters. A rough scan over this parameter space (e.g. choosing either small, medium and large for each parameter) needs $3^{120} \approx 2.10^{57}$ simulations. At a rate of one simulation per µs (very optimistic), one would need 5.10^{43} year. Hence it is primordial to pin some parameters at the beginning. These can be obtained by scanning the available literature and minute analysis of distinct measurements performed on the studied cell.

One cannot measure everything. Hence one is obliged to choose some parameters as commonly reported in literature. Usually the exact values of these parameters are not the real interest of the modeler (e.g. the relative dielectric permittivity), or else very hard to measure (e.g. band alignment between buffer and absorber).

Unfortunately there can be some spread on the reported results. This is amongst others the case for the band gap dependency with respect to the composition of CIGS. Combining the reports of several authors ([9], [10], [11], [12]) about the band gap of $Cu(In,Ga)Se_2$, $Cu(In,Ga)S_2$, $CuIn(Se,S)_2$ and $CuGa(Se,S)_2$ we can however derive the band gap dependency for $Cu(In_{1-y},Ga_y)(Se_{1-x},S_x)_2$.

$$E_g[eV] = -0.14x^2y + 0.14x^2 + 0.39xy + 0.15y^2 + 0.35x + 0.49y + 1.04 \quad (1)$$

Or, with rearrangements,

$$E_g[eV] = 1.04(1-x)(1-y) + 1.68(1-x)y + 1.53x(1-y) + 2.42xy - 0.14x(1-x)(1-y) - 0.15y(1-y) \quad (2)$$

where one better recognizes the band gaps of the ternary materials $CuInSe_2$, $CuGaSe_2$, $CuInS_2$ and $CuGaS_2$.

This kind of formula can now also be used for example to extract In/Ga-ratio or the Se/S-ratio when the Se/S-ratio respectively the In/Ga-ratio is already known.

Next to numerical data also rules of thumb can be found in literature. For band gap grading a rule called ‘the common anion/cation rule’ is often used. This states that if one changes the In/Ga ratio (common anion rule) there will be a band gap change due to a change in the conduction band (CB). Analogously changing the S/Se ratio (common cation rule) will lead to a band gap change due to a change in the valence band (VB).

3 CLUES FROM MEASUREMENTS

When one sticks to literature data, one gets a ‘typical solar cell’ model. Adding measurement data makes it realistic. The more different measurements one uses the better. For the model described here we used *C-V*, *C-f* and *I-V* measurements at different temperatures next to spectral response and DLTS measurements. Additionally we used SIMS measurements reported in [2]. These show the cell has a ‘front grading’ with sulphur which will result in a valence band lowering according to the common cation rule, and a gallium ‘back grading’ resulting in a conduction band raise. This is represented in Fig. 1.

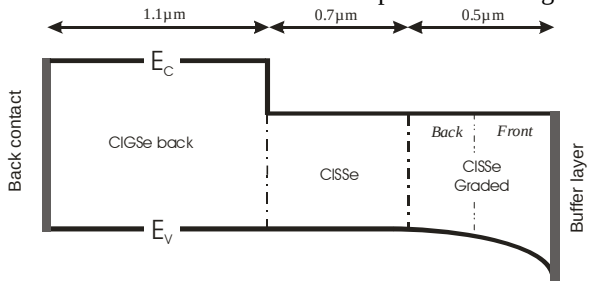

Figure 1: Schematics of the absorber layer band structure. The absorber-backcontact interface is on the left hand side, the interface with the buffer on the right hand side. There are 4 layers: *CIGSe back* models the back Ga-grading; *CISSe graded* models the front S-grading and is splitted in 2 parts (*Back* and *Front*); *CISSe* makes the transition between the back and the front grading.

3.1 A graded band gap

A straightforward way for determining the band gap is the measurement of the spectral response (see Fig. 2). Only photons with an energy higher than the absorber band gap will give a contribution to the photocurrent. This way we were able to determine the *optical* band gap of the absorber as approximately 1.0 eV.

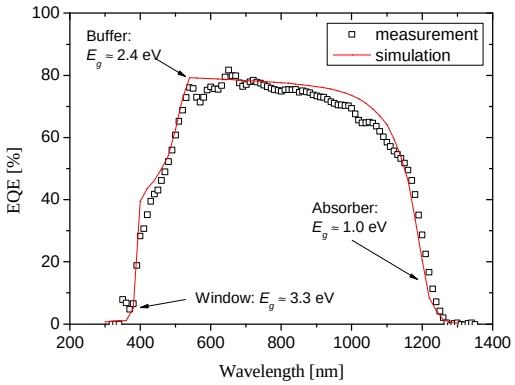

Figure 2: External quantum efficiency plot. The band gaps of buffer, window and absorber can be seen in the different transitions in the plot. The optical band gap of the absorber is approximately 1.0 eV.

A second way of determining the band gap is extrapolating the value of V_{oc} for $T = 0$ K. In the case of bulk recombination (which is the most important in modern devices) this open circuit voltage can be interpreted as: $E_g = qV_{oc}$ [13]. Performing this analysis (see Fig. 3) we end up with a *recombination* band gap value of about 1.1 eV.

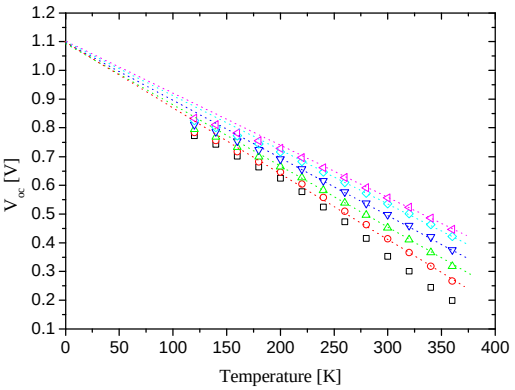

Figure 3: V_{oc} as a function of temperature measured under different light power conditions. Extrapolation to $T = 0$ K leads to a recombination band gap of about 1.1 eV.

It appears that the values of the optical and recombination band gap do not agree. This is due to the grading of the sample. The optical band gap is determined by the minimum band gap of the absorber, in our sample occurring in the middle of the layer. The recombination band gap can be related to the band gap at the place where most of the recombination happens, usually in the space charge region (SCR). This is in accordance with the SIMS

measurements predicting a raise of the band gap towards the SCR due to S-incorporation.

We can now use the measured band gaps together with the SIMS data to determine the composition of the CIGS throughout the absorber. According to formula (1), a band gap of 1.1 eV corresponds with $CuIn(Se_{0.84},S_{0.16})_2$ in the $CuIn(S,Se)_2$-system. A band gap of 1.0 eV corresponds with almost pure $CuInSe_2$. Here the fact that literature data should be handled with care is again emphasized, as the minimum band gap of CIGS according Eq. (1) is 1.04 eV rather than the measured 1.0 eV. We thus start with a frontgrading ranging from S/(Se+S) = 0 to S/(Se+S) = 0.16. Afterwards we refined these values to respectively 0.1 and 0.3 in order to get a better agreement between the measured and simulated spectral response curve.

3.2 Defect properties

The electrical properties of defect levels within the band gap of the absorber have been measured by means of DLTS. For these cells three different levels could be distinguished, shown in Fig. 4.

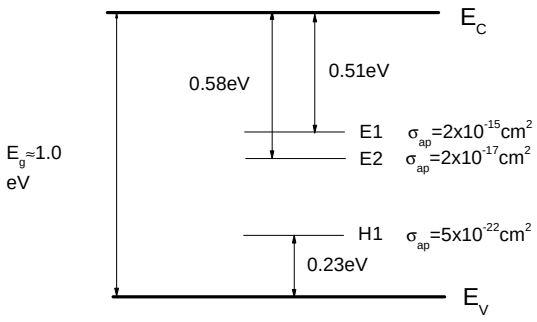

Figure 4: Graphical view of the defect levels observed by means of DLTS within the graded part of the band gap. The band gap corresponds to the recombination band gap, as explained in the previous section.

Two of them labeled E1 and E2 were observed as minority carrier traps and thus only visible by applying a forward injection pulse (V_p = 0.5 V). The apparent activation energy is observed with respect to the conduction band and the apparent capture cross-section is for electrons. With conventional DLTS reverse biased only a single level H1, 0.23 eV above the valence band could be observed with a small capture cross-section for holes.

We should now introduce the observed defects in our model. However, not all of them, but only those who really influence the cell behaviour, should be modelled. In the model we should thus have two more or less midgap defects with a cross section around 10^{-15}-10^{-17} cm^2. In the final model these appear as *Defect 2* and *Defect 3*, see Table 1.

3.3 Apparent doping

C-V measurements result in an apparent doping profile of the least doped part of the junction (in our case the absorber part). The results from this measurement are shown in Fig. 5. This way we can get a clue about the charge distribution throughout the absorber. If there is some grading present, we can see it straightaway.

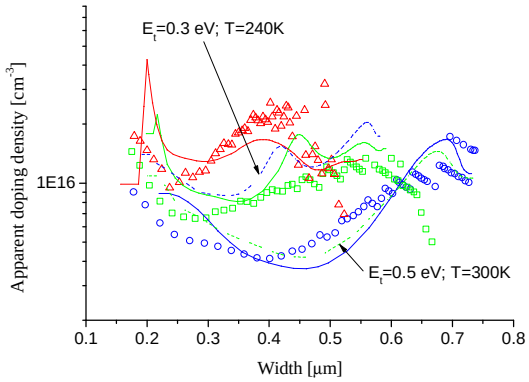

Figure 5: Apparent doping density at *T*=240-300-360 K (blue circles-green squares-red triangles). Measurement data marked with symbols, the simulation data of the final model in solid lines. In dashed lined the simulation results are shown if the energy level of *Defect 2* is changed as discussed in § 4. All *C-V*-measurements and simulations performed at 10 kHz.

As can be seen in Fig. 5, increasing the temperature increases the charge density at a depth of about 0.4 µm. This could be due to acceptor defects at this depth. Together with the results of the previous section we now have as a starting point for the model a good guess about the defect density distribution and the energy level of the defects. To be able to reproduce the measured apparent doping profiles for all temperatures however, a good deal of refinement is still necessary. A lot of parameters come into play here. The capture cross-sections, the exact energy level and the density distribution of the various defects in the different layers, together with the shallow doping density… The result of the optimization is also shown in Fig. 5.

4 OPTIMIZING THE MODEL

As stated above, literature and measurements give a good clue about the interior of the cell, but in order to get a really good model things have to be

optimized. This optimization can, as explained, not be performed automatically. According to the problem, each measurement has a different relative importance which can only be estimated by the modeler himself. Next to this, a good understanding of semiconductor physics and simple rules of thumb is indispensable to optimize the model.

In Fig. 5 an example of the optimization of the energy level of a defect is shown. To get the best agreement between simulation and measurements for the *C-V*-curves it seems that the energy level of this defect (defect 2 in Table 1) should be 0.4 eV above the VB. Changing this level to e.g. 0.3 eV or 0.5 eV breaks the agreement with measurement for T=240 K and T=300 K respectively. This way we can pin this energy level in a rather short range.

Care should however be taken. Changing this level also influences other measurement fits (e.g. *C-f*). Additionally, other parameters can have a similar or counteracting effect (e.g. the capture cross section of the defect or the properties of other defects).

5 THE FINAL MODEL

The final model consists of 6 different layers: a 0.2 µm thick ZnO-window layer, a 0.1 µm thick CdS-buffer layer and 4 layers modelling the 2.3 µm thick absorber. The absorber is represented in Fig. 1. At the back of the absorber there is a layer with extra gallium (*CIGSe back*) consisting of $Cu(In_{0.6},Ga_{0.4})Se_2$. At the front there is an exponential front grading with sulphur (*CISSe graded*). This front grading ranges from S/(Se+S) = 0.3 at the absorber-buffer-interface to 0.1 at the back of the graded layer. In between there is a transition-background layer (*CISSe*). The *CISSe graded*-layer is split up in two different parts, 'back' and 'front', the front part is 50% thicker than the back part. They only differ with respect to shallow doping and defect properties. All defect and doping properties are summarized in Table 1. The agreement between the measurements and the simulation are shown in Fig. 2, 5 and 6.

Additionally, we simulated the occupation of *Defect 2* for reverse biased and injection pulse conditions. It could be seen that the corresponding capacitance transient originates in the emission of electrons. This observation is in very good agreement with the sign of the DLTS signal of the main (i.e. the defect with the highest capacitance transient amplitude) defect E2, which is a minority carrier trap.

	CISSe	CISSe graded back	CISSe graded front
N_A [cm^{-3}]	5 10^{15}	5 10^{14}	10^{16}

Defect 1		*neutral*	
σ_n [cm^2]	10^{-15}	10^{-15}	10^{-15}
E_t	E_i	E_i	E_i
N_T [cm^{-3}]	10^{15}	10^{15}	10^{15}
L_n [µm]	5.6	5.6	5.6
Defect 2		*acceptor*	
σ_n [cm^2]	10^{-14}	10^{-15}	10^{-15}
E_t [eV]	0.4	0.4	0.4
N_T^{left} [cm^{-3}]	10^{16}	2 10^{16}	5 10^{15}
N_T^{right} [cm^{-3}]	10^{16}	5 10^{15}	5 10^{15}
L_{char} [µm]	#	0.05	#
L_n [µm]	0.56	1.2	2.5
Defect 3		*acceptor*	
σ_n [cm^2]	#	#	10^{-15}
E_t [eV]	#	#	0.55
N_T [cm^{-3}]	#	#	1.3 10^{16}
L_n [µm]	#	#	1.5

Table 1: Parameters used to define doping and defect distribution in the front part of the absorber: N_A: shallow doping density; σ_n: capture cross section of electrons; N_T: defect density; L_n: electron diffusion length. *Defect 2* has an exponential distribution in the back part of the CISSe graded layer, hence the left and right concentration is mentioned, L_{char} is the characteristic length. *Defect 3* is only present in the front part of the CISSe graded layer. Energy levels (E_t) are referred with respect to the VB, unless they are on the intrinsic level: E_i. The CIGSe back layer has a shallow doping concentration of 1.7 10^{16} cm^{-3}. Only defect 1 is present in this layer with a concentration of 10^{15} cm^{-3} and a cross section of 10^{-15} cm^2. *Defect 2* and *Defect 3* are acceptor levels and correspond to the defects measured by DLTS. *Defect 1* is a neutral defect and is only used to set a background recombination.

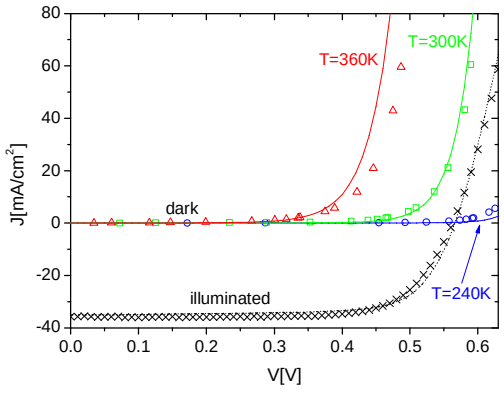

Figure 6: measured (symbols) and simulated (solid lines) current voltage characteristics. Dark characteristics at T=240-300-360 K. Illuminated characteristic at room temperature under AM1.5 conditions.

6 SETTING THE BACKGROUND

The big advantage of numerical modelling of graded solar cells is the fact one can discern the benefit of the grading from other influences.

When one changes the grading of a parameter throughout the solar cell one does not only change the shape of the grading, but usually also the mean value of this parameter. To really understand the influence of the grading, and not of the change in mean value of the parameter one should always compare the sample with a uniform sample, where the graded parameter is averaged out. In real life this is impossible, it is already hard to make two cells identical. But in a numerical model this is already a lot easier.

However, care should be taken. If one for example wants to investigate the grading depth by increasing a layer width (and decreasing another, to keep the total width constant) one should be aware that one changes a lot of other properties as well, e.g. adding defects at a specific place in the absorber which are present in one layer but not in the other

Determining real grading benefits is thus a rather complicated task. One should realize the work is certainly not finished once the model has been constructed. Perhaps the toughest barrier then still has to be overcome: determining which parameters are really due to the grading and which not. An example of such an analysis can be found in [14].

7 CONCLUSIONS

To be able to understand the effect of band gap grading on solar cells numerical simulation is a very useful, if not indispensable, tool. As the net effect of grading is dependant on a lot of parameters a very realistic model is needed. We showed how starting from literature data and measurement results such a model can be built in SCAPS.

To be able to discern the net effect of grading, one should compare simulation results with those of a uniform reference.

Acknowledgments

We acknowledge the support of the Research Foundation – Flanders (K.D., FWO Ph. D. Fellowship), of the European Integrated project 'Athlet'. We thank AVANCIS (München, Germany) for providing CIGS cell samples.

References

[1] O. Lundberg, M. Edoff, L. Stolt, "The effect of Ga-grading in CIGS thin film solar cells", Thin Solid Films, vol. 480-481, pp. 520-525 , 2005.

[2] J. Palm, V. Probst, F.H. Karg, "Second generation CIS solar modules", Solar Energy, vol. 77, pp. 757-765, 2004.

[3] M. Topič, F. Smole, J.Furlan, "Band-gap engineering in CdS/Cu(In,Ga)Se_2 solar cells", J. Appl. Phys., vol. 79, no. 11, pp. 8537-8540, 1996.

[4] A.M. Gabor, J.R. Tuttle, M.H. Bode, A. Franz, A.L. Tennant, M.A. Contreras, R. Noufi, D.G. Jensen, A.M. Hermann, "Band-gap engineering in Cu(In,Ga)Se_2 thin films grown from $(In,Ga)_2Se_3$ precursors", Sol. Energy Mater. Sol. Cells, vol. 41-42, pp. 247-260, 1996.

[5] M. Gloeckler, Device physics of Cu(In,Ga)Se2 thin-film solar cells, Ph.D. thesis, Colorado State University, Fort Collins, 2005.

[6] M. Burgelman, J. Verschraegen, S. Degrave and P. Nollet, "Modeling thin film PV devices", Progress in Photovoltaics, vol. 12, pp. 143-153, 2004.

[7] M. Burgelman, P. Nollet and S. Degrave, "Modelling polycrystalline semiconductor solar cells", Thin Solid Films, vol. 361-362, pp. 527-532, 2000.

[8] M. Burgelman, J. Marlein, "Analysis of graded band gap solar cells with SCAPS", in: Proceedings of the 23rd European Photovoltaic Conference, Valencia, Spain, 2008, pp. 2151-2155.

[9] S.J. Fonash, "Solar Cell Device Physics", Academic Press, San Diego, 1981.

[10] H. Neff, P. Lange, M.L. Fearheiley, K.J. Bachmann, "Optical and electrochemical properties of $CuInSe_2$ and $CuInS_2$- $CuInSe_2$ alloys", Appl. Phys. Lett., vol. 47, no. 10, pp. 1089-1091, 1985.

[11] M. Turcu, I.M. Kötschau, U. Rau, "Composition dependence of defect energies and band alignments in the $Cu(In_{1-x},Ga_x)(Se_{1-y}S_y)_2$ alloy system", J. Appl. Phys., vol. 91, no. 3, pp. 1391-1399, 2002.

[12] S. Wei, A. Zunger, "Band offsets and optical bowings of chalcopyrites and Zn-based II-VI alloys", vol.78, no. 6, pp.3846-3856, 1995.

[13] U. Rau, H.W. Schock, "Cu(In,Ga)Se_2 Solar Cells", Ch. 7 in "Clean Energy from Photovoltaics", edited by M.D. Archer and R. Hill, Imperial College Press, London, 2001.

[14] K. Decock, J. Lauwaert, M. Burgelman, "Characterization of graded CIGS solar cells", presented at the E-MRS spring meeting 2009, symposium B, Strasbourg, 2009.